

Task 55 Towards the Integration of Large SHC Systems into DHC Networks

B-D1.1 Application of PC Method to Large Collector Arrays

IEA SHC FACT SHEET 55 B-D1.1

Subject:	Application of Performance Check (PC) Method to Large Collector Arrays
Description:	The Performance Check (PC) method can be used for a simple check of the collector array performance of a solar thermal plant. It has been proposed recently as an input to a new ISO standard. This fact sheet provides an application of the PC method to large collector arrays. The goal of this fact sheet is to evaluate the methodology and provide practical insights for the application of the PC method.
Date:	12.02.2021
Authors:	Daniel Tschopp (AEE INTEC), Pierre Delmas (newHeat), Mathieu Rhedon (newHeat), Sacha Sineux (newHeat), Alexis Gonnelle (newHeat), Philip Ohnewein (AEE INTEC), Jan Erik Nielsen (PlanEnergi)
Download possible at:	http://task55.iea-shc.org/fact-sheets

Content

Introduction.....	2
Performance Check (PC) method	2
Equations	2
Performance measurement	3
Data selection	4
Uncertainty levels	4
Results.....	4
Application to plant <i>Fernheizwerk</i> (Graz, Austria)	5
Plant description and measurement setup.....	5
Data handling and uncertainties	7
Performance analysis	11
Discussion of results.....	18
Application to plant <i>Condat Paper Mill</i> (Condat-sur-Vézère, France)	19
Plant description and measurement setup.....	19
Data handling and uncertainties	21
Performance analysis	22
Discussion of results.....	24
Conclusion and outlook.....	25
Nomenclature.....	27
References	28

B-D1.1 Application of PC Method to Large Collector Arrays

Introduction

Performance checks and guarantees for large-scale solar thermal systems are an increasingly important tool to minimize the risk associated with building a solar thermal plant [1]. The development of in situ test methods is currently investigated in numerous research projects [2]. A simple and easy applicable method to check the thermal power output for large collector arrays is the Performance Check (PC) method. It has been used in Denmark for approximately 10 years. The method has undergone revisions. The first version was described in IEA-SHC TECH SHEETS 45.A.3.1. [3].

Recently, it has been proposed as an input to a new ISO standard and a working group under ISO/TC 180 is elaborating the standard right now [5]. IEA SHC Task 55 Fact Sheet *B-D2 Collector fields – Check of performance* provides a detailed description of how to guarantee the collector field power performance. IEA SHC Task 55 Fact Sheet *B-D1.2 Review of In Situ Test Methods for Solar Collectors and Solar Collector Arrays* gives a comparison of the PC method with two other test methods, namely *In situ Collector Certification (ICC)* and *Dynamic Collector Array Test (D-CAT)*.

This fact sheet describes the application of the PC method to two solar thermal plants in order to evaluate the methodology and provide practical insights for its application. The first plant is *Fernheizwerk*, located in Graz (Austria), where the method is applied to four subarrays with flat plate collectors of different collector manufacturers. The second plant is *Condat Paper Mill*, located in Condat-sur-Vézère (France), which uses a one-axis tracking system for flat plate collectors, for the first time on a large-scale.

Performance Check (PC) method

A short summary of the method is given below. The overall principle of the PC method is to check the measured power against the estimated power when the collector array is running close to full power. Hence, the PC methodology can be categorized as static. It can be used in connection with commissioning of the collector array and/or for continuous on-line surveillance. Flat plate and concentrating collector arrays can be tested.

Equations

The estimated power is calculated based on collector parameters from ISO 9806 [6] plus some safety factors. These collector parameters are typically available for solar thermal collectors on the market. The equation used for estimating the collector array power is chosen depending on the collector type and targeted uncertainty level. Three equations are available:

Equation A: A simple power performance estimate for non-concentrating collectors:

$$\dot{Q}_{\text{sec,est}} = A_G \cdot [\eta_{0,\text{hem}} G_{\text{hem}} - a_1 (\vartheta_m - \vartheta_a) - a_2 (\vartheta_m - \vartheta_a)^2 - a_5 (d\vartheta_m / dt)] \cdot f_{\text{safe}} \quad (\text{eq. A})$$

Task 55 Towards the Integration of Large SHC Systems into DHC Networks

B-D1.1 Application of PC Method to Large Collector Arrays

Equation B: A more advanced equation for non- or low-concentrating collectors (concentration ratio $C_R < 20$) can be used if the direct and diffuse radiation on the collector plane is available. Using eq. B will normally give results with smaller uncertainty than using eq. A as incidence angle modifiers for the collector are considered in eq. B.:

$$\dot{Q}_{\text{sec,est}} = A_G \cdot [\eta_{0,b} K_b(\theta_L, \theta_T) G_b + \eta_{0,b} K_d G_d - a_1 (\vartheta_m - \vartheta_a) - a_2 (\vartheta_m - \vartheta_a)^2 - a_5 (d\vartheta_m/dt)] \cdot f_{\text{safe}} \quad (\text{eq. B})$$

Equation C: Is used for concentrating collectors with high concentration ratio $C_R \geq 20$ – tracking in one or two axis and utilizing mainly or only direct radiation (effectively, diffuse radiation conversion is set to zero):

$$\dot{Q}_{\text{sec,est}} = A_G \cdot [\eta_{0,b} K_b(\theta_L, \theta_T) G_b - a_1 (\vartheta_m - \vartheta_a) - a_2 (\vartheta_m - \vartheta_a)^2 - a_5 (d\vartheta_m/dt) - a_8 (\vartheta_m - \vartheta_a)^4] \cdot f_{\text{safe}} \quad (\text{eq. C})$$

f_{safe} is taking into account pipe and other heat losses (f_p), measurement uncertainty (f_u) and other uncertainties (f_o). When all factors are detailed, it can be calculated with: $f_{\text{safe}} = f_p \cdot f_u \cdot f_o$. The selected values are typically agreed upon contractually between a supplier and its client.

Performance measurement

Although the performance is checked for the primary loop, it is recommended to measure the power output on the secondary side of the heat exchanger to avoid uncertainties originating from the physical properties of the collector loop fluid. The thermal power of the collector array $\dot{Q}_{\text{sec,meas}}$ is based on volume flow and temperature measurements:

$$\dot{Q}_{\text{sec,meas}} = \dot{V}_{\text{L,SEC}} \cdot \rho_{\text{i,sec}} \cdot C_{f,\text{sec}} (\vartheta_{\text{e,sec}} - \vartheta_{\text{i,sec}})$$

The necessary measurement equipment for the radiation depends on the used equation

- *Eq. A:* Global irradiance measurement in the collector plane is needed.
- *Eq. B:* Direct and diffuse irradiance measurement is needed. Options are:
 - Pyranometer for global irradiance in the collector plane + pyranometer with shadow ring for diffuse irradiance in the collector plane
 - Pyranometer for global irradiance in collector plane + pyrhelimeter for beam irradiance
- *Eq. C:* Only pyrhelimeter for beam irradiance is needed.

Other measurement sensors:

- Energy meter (flow meter and temperature sensors or combined unit, measured in secondary / water loop)
- Temperature sensors for in- and outlet of heat exchanger primary loop
- Temperature sensor for ambient air temperature
- Anemometer for wind velocity

Logging / recording:

- Measurement data are logged (and calculated) at least each minute. These data are then averaged and recorded for each hour. The values in the record shall represent the average values over the last hour.

Task 55 Towards the Integration of Large SHC Systems into DHC Networks

B-D1.1 Application of PC Method to Large Collector Arrays

Data selection

To limit uncertainties, some restrictions on the operating conditions are given (Table 1). Only measurement points which satisfy these restrictions are valid and can be used as input data to the method.

Table 1: Restriction on operating conditions

Operating condition	Limits		
	Eq. A	Eq. B	Eq. C
Shadows	No shadows		
Incidence angle	$\leq 30^\circ$	-	-
Change in collector mean temperature	≤ 5 K (within 1 hour)		
Ambient temperature	≥ 5 °C		
Wind velocity	≤ 10 m/s		
G_{hem}	≥ 800 W/m ²	-	-
G_b	-	≥ 600 W/m ²	≥ 600 W/m ²

Only data records (hourly average values) fulfilling the requirements (see Table 1) are valid. For checking the collector performance, the measuring period shall have at least 20 data records.

Uncertainty levels

The present version of the method has two levels of uncertainty:

- Level I: Measured solar radiation: ± 3 % and power output ± 2 %
- Level II: Measured solar radiation ± 5 % and power output ± 3 %

Results

- The main results/indicators of the method are key figures that show the deviation in performance between measurement and calculation (expected performance based on data sheet parameters):

$$d\dot{Q}\% = (\dot{Q}_{sec,meas} - \dot{Q}_{sec,est}) / \dot{Q}_{sec,meas}$$

- These figures are:
 - One figure giving a comparison of all measured power points with the corresponding calculated/estimated power point (see Figure 16 as an example)
 - One figure summarizing all the measured power points with all the calculated/estimated power points given as a percentage (the calculated/estimated sum being set as 100% - the measured sum being then a bit higher or lower) (similar to Figure 18, but with percentage values)

Task 55 Towards the Integration of Large SHC Systems into DHC Networks

B-D1.1 Application of PC Method to Large Collector Arrays

Application to plant *Fernheizwerk (Graz, Austria)*

Plant description and measurement setup

The plant data is listed in Table 2.

Table 2: Basic data of plant *Fernheizwerk*

<i>Overview</i>	
Name	Fernheizwerk
Location	Graz (Austria)
Latitude, longitude	47.05° N, 15.44° E
Operation start	2014/2015
Application	Feed-in to district heating network of the City of Graz
System integration	Return/Supply connection with DH network
Plant operator	SOLID Solar Energy Systems GmbH
<i>Collector array</i>	
Collector type	2 subarrays with flat plate collectors - single-glazed and foil, 2 subarrays with flat plate collectors - double-glazed
Collector manufacturer	KBB Kollektorbau, GREENoneTEC, Arcon, ÖkoTech Solarkollektoren
Collector model	K5Giga+ (KBB), GK 3133 (GoT), HTHEATstore 35/10 (Arcon), ökoTech HT 12.5 (ÖkoT)
Absorber type	harp (3 subarrays), meander (1 subarray)
Collector efficiency parameter (Solar Keymark)	$\eta_{0,b}$: 0.72 to 0.76; b_0 : 0.15 to 0.22; $K_d(50^\circ)$: 0.86 to 0.87; a_1 : 1.97 to 2.66 W/(K·m ²); a_2 : 0.006 to 0.015 W/(K ² ·m ²); a_5 : 7,313 to 15,140 J/(K·m ²)
Collector gross area	12.4 to 13.6 m ²
Total gross collector area	1,538 m ² (all 4 subarrays)
Slope	30°
Orientation	180° (south)
Row spacing	3 m
Fluid	primary loop: propylene glycol (43.5%) (used for performance assessment); secondary loop: water
<i>Measurement setup</i>	
Volume flow (primary side)	Electromagnetic flow sensor OPTIFLUX 4000 DN32 IFC 100
Fluid temperature	Resistance Thermometer Pt100 (EN 60751 F.01), placed directly in fluid (without thermowell)
Ambient temperature	Resistance Thermometer Pt100 (EN 60751 F.01), with ventilation unit
Fluid properties	Laboratory test for density and heat capacity by ILK Dresden (maximum error +/- 0.5% for fluid density, +/- 1% for heat capacity)
Total radiation in collector plane	Pyranometer Kipp & Zonen SMP 21
Beam radiation (DNI)	Pyrheliometer Kipp & Zonen SHP1 (mounted on Kipp & Zonen SOLSYS 2 sun tracker)
Wind speed (horizontal)	Ultrasonic Wind Sensor Lufft V200A-UMB
Data logging	PLC B&R Industrial Automation X20CP1483, four wire (4 L) connection to temperature sensors
Sampling rate	1 second
Measurement quality assurance	regular on-site inspection of measurement equipment, regular cleaning of radiation sensors, automated checks for data transmission, missing data and physically implausible values, documentation of all plant events (e.g. power supply interruption, maintenance work, etc.)

Task 55 Towards the Integration of Large SHC Systems into DHC Networks

B-D1.1 Application of PC Method to Large Collector Arrays

Data evaluation

Measurement period	2017-01-01 to 2017-12-31 (subtracting two weeks of missing data / operation interruption)
Evaluation tool	Data evaluation tool developed by AEE INTEC based on MATLAB® [7]
Used equation for PC method	eq. A, eq. B
Evaluation performed by	AEE INTEC

The plant *Fernheizwerk* provides heat to the district heating network of Graz. It is located in close proximity to the gas-fired district heating plant FHW (*Fernheizwerk*), where the plant takes its name from. The solar thermal plant is separated from the grid by two heat exchangers and feeds directly into the grid, there is no storage. The solar circuit consists of two separated collector arrays with a total gross collector area of 8,249 m². One of these collector arrays, depicted in Figure 1, is located on a grass field. It was equipped with high precision measurement equipment within the research project *MeQuSo*. Further information on the plant is available in the project report [8].



Figure 1: Collector array of plant *Fernheizwerk*. Source: Picfly.at Thomas Eberhard

The PC method was applied to four subarrays with gross collector areas of 211 m², 400 m², 516 m² and 523 m² respectively. Each subarray has flat plate collectors of a different collector manufacturer installed. Figure 2 shows the hydraulic layout of the array and the position of the measurement sensors. All subarrays are in the same hydraulic circuit. They have similar return temperatures and are controlled for the same outlet temperature. Each of the four subarrays has a volume flow, return and flow temperature sensor, which allows to calculate the thermal power output of each subarray separately. Although the PC method recommends to measure the thermal power output on the secondary side due to fluid property uncertainties pertaining to heat transfer mediums other than water, it is unproblematic here, as a laboratory test for the fluid properties has been conducted (which indeed showed significant differences for the heat capacity values [8]). Results of the subarrays are anonymized (collector array #1 to collector array #4).

Task 55 Towards the Integration of Large SHC Systems into DHC Networks

B-D1.1 Application of PC Method to Large Collector Arrays

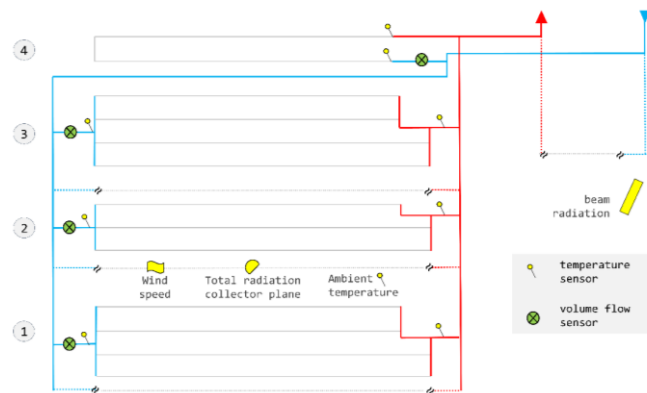


Figure 2: Hydraulic scheme and measurement setup of plant *Fernheizwerk*. Source: SOLID, adapted by AEE INTEC

Data handling and uncertainties

Data acquisition and pre-processing

Measurement data was recorded with a sampling rate of 1 second. In the first step, the calibration correction was applied. Data outside physically plausible ranges (e.g. ambient temperatures above 50 °C, negative volume flows, etc.) were discarded by automated checks. Missing data with a maximum time gap to the next observation of 1 minute were interpolated linearly. Data was then resampled to 1 min. mean values. Additional data checks based on the Input-Output method [9] and time series plots were performed to validate the measurement setup. All data was recorded in standard time during the whole measurement period. The logger was periodically checked for a potential time drift and radiation peaks on clear days were inspected if they match noon of true solar time. Beam incidence angles were calculated according to [10].

Internal and external shading

As the row spacing is very narrow (3 m), internal shading plays a crucial role. As stated in Table 1, data are required to be without shading. To select data without internal shading, an algorithm based on [11] was implemented; the algorithm calculates the shadow length on a collector row. External shading was also a major issue. Towards west, the transport pipe of the district heating grid with a height of approx. 3 m passes the collector array in close distance and towards south and west there are buildings and trees within 20 to 50 m distance. Given the closeness of the shading objects and the large area occupied by the collector arrays of around 60 m x 90 m, external shading was inhomogeneous. This made the consideration of the 3D topography necessary. A 3D model was set up in *SketchUp* (see Figure 3) as part of a master thesis at AEE INTEC [12].

Task 55 Towards the Integration of Large SHC Systems into DHC Networks

B-D1.1 Application of PC Method to Large Collector Arrays



Figure 3: SketchUp model of collector array of plant *Fernheizwerk*. Source: AEE INTEC

The basic 2D aerial picture to build the model was imported from Google Earth and complemented with building heights from a local GIS provider [13]. The height of the trees was calculated based on measurements of the position relative to reference points and the view angle measured by an angle measurement device. Based on the SketchUp model, for each day the first time point where external shading stops in the morning for all subarrays and the last time point where external shading begins in the afternoon for at least one array was determined with the built-in shadow function of the program, which visually displays shadows for manually selectable times. The external shading pattern was regular in the sense that between these two time points, there were no intermittent periods with external shading. The start and end time points were then visually validated with pictures of a webcam installed on-site, which showed a good agreement.

The results are shown in Figure 4. Plant operation where no internal and external shading occurs is between the 23rd of March and 23rd of September. The total hours without shading amount to 1,348 h a year. As can be seen, the restriction that there should be no shading can significantly reduce the valid data for the PC method.

B-D1.1 Application of PC Method to Large Collector Arrays

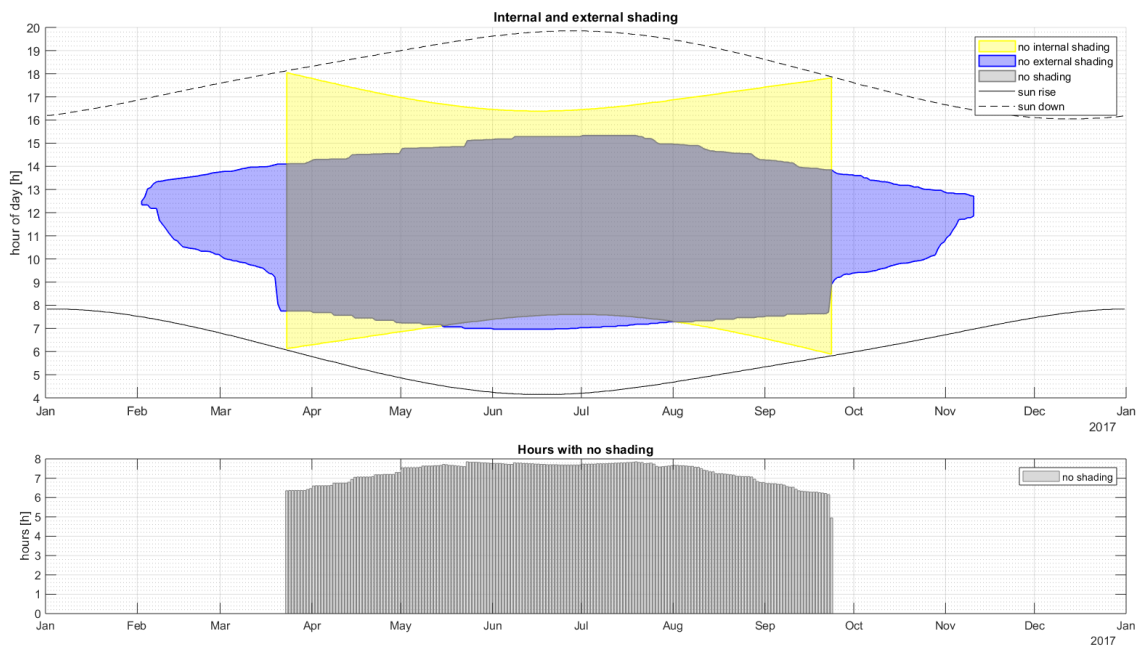


Figure 4: Internal and external shading of plant *Fernheizwerk*. The core area labelled “no shading” marks the data intervals that can be used for the PC method

Uncertainties

The PC method lists three types of uncertainties, namely heat losses from pipes f_p , measurement uncertainties f_U and other uncertainties f_o (non-ideal flow distribution, unforeseen heat losses, uncertainties in the model/procedure).

For the investigated collector arrays, heat losses from pipes are very small, because the temperature sensors are placed just before the first and after the last collector of the subarray. Regarding other uncertainties, losses from non-uniform flow distribution should also be very small, as an analysis of the outlet temperatures on a row-by-row basis showed a good agreement between rows and as efficiency losses for fairly balanced collector arrays are low [14]. Unforeseen heat losses are also estimated to be small. Heat exchanger losses do not apply for the measurement setup. Some uncertainties in the model/procedure are addressed in the sections “Performance analysis” (p. 11ff.) and “Discussion of results” (p. 16ff.).

Measurement uncertainties for the deployed sensors were determined based on data sheet specifications of the manufacturer (see Table 2). Multiple uncertainty sources for a particular sensor (e.g. zero off-set, long term stability, non-linearity and temperature dependence for pyranometer measurements) were combined to a sensor uncertainty expressed as a standard deviation of a normal distribution according the *Guide to the expression of uncertainty in measurement* (GUM) [15]. Further recommendations of the application of the GUM method to collector array measurements can be found in [16].

Measurement uncertainties depend on the operating point. Table 3 shows measurement uncertainties for the operating points which correspond to the average of all valid data records of collector array #1 for eq. A

Task 55 Towards the Integration of Large SHC Systems into DHC Networks

B-D1.1 Application of PC Method to Large Collector Arrays

and eq. B respectively. As shown, the measurement uncertainties for the power output are lower than +/- 2%. Also, the uncertainties for the solar radiation measurements are lower than +/- 3% (not shown in the table). Therefore, the evaluation achieves the accuracy level I as defined by the PC method. Uncertainties of collector parameter values were not taken into account for the estimated output.

Table 3: Measurement uncertainties of plant *Fernheizwerk*

	Mean of valid data records	+/- 2σ ¹⁾	Uncertainty sources ²⁾
eq. A³⁾			
$\dot{Q}_{\text{meas,pri}} / A_G$	497.9 W/m ²	+/- 9.0 W/m ² (+/- 1.8%)	$\dot{V}_{i,\text{pri}} = 5.5\%$, $\rho_{i,\text{pri}} = 10.3\%$, $c_{t,\text{pri}} = 41.1\%$, ϑ (all) = 43.2%
$\dot{Q}_{\text{est,pri}} / A_G$	469.4 W/m ²	+/- 11.8 W/m ² (+/- 2.5%)	$G_{\text{hem}} = 99.0\%$, ϑ (all) = 1.0%
$\dot{Q}_{\text{meas,pri}} / \dot{Q}_{\text{est,pri}}$	106.1%	+/- 3.2%	$G_{\text{hem}} = 65.6\%$, $\dot{V}_{i,\text{pri}} = 1.9\%$, $\rho_{i,\text{pri}} = 3.5\%$, $c_{t,\text{pri}} = 14.0\%$, ϑ (all) = 15.1%
eq. B⁴⁾			
$\dot{Q}_{\text{meas,pri}} / A_G$	490.5 W/m ²	+/- 8.9 W/m ² (+/- 1.8%)	$\dot{V}_{i,\text{pri}} = 5.4\%$, $\rho_{i,\text{pri}} = 10.1\%$, $c_{t,\text{pri}} = 40.6\%$, ϑ (all) = 43.8%
$\dot{Q}_{\text{est,pri}} / A_G$	457.4 W/m ²	+/- 10.8 W/m ² (+/- 2.4%)	$G_{\text{hem}} = 98.7\%$, $G_b = 0.1\%$, ϑ (all) = 1.2%
$\dot{Q}_{\text{meas,pri}} / \dot{Q}_{\text{est,pri}}$	107.2%	+/- 3.2%	$G_{\text{hem}} = 62.5\%$, $G_b = 0.1\%$, $\dot{V}_{i,\text{pri}} = 2.0\%$, $\rho_{i,\text{pri}} = 3.8\%$, $c_{t,\text{pri}} = 15.0\%$, ϑ (all) = 16.7%

¹⁾ σ = standard deviation; value ± 2σ is equal to a 95.45% confidence interval for a normal distribution

²⁾ Contribution to uncertainty of measurand X_i for calculated value Y : $(dY/dX_i)^2 \cdot u(X_i)^2 / u^2(Y)$

³⁾ for average conditions of eq. A valid data records ($\dot{V} = 15.4 \text{ l}/(\text{h} \cdot \text{m}^2)$, $\vartheta_i = 69.7^\circ \text{C}$, $\vartheta_e = 99.2^\circ \text{C}$, $\vartheta_a = 25.9^\circ \text{C}$, $G_{\text{hem}} = 964.2 \text{ W}/\text{m}^2$, $d\vartheta_m/dt = 0.43 \text{ K}/\text{h}$)

⁴⁾ for average conditions of eq. B valid data records ($\dot{V} = 15.4 \text{ l}/(\text{h} \cdot \text{m}^2)$, $\vartheta_i = 69.5^\circ \text{C}$, $\vartheta_e = 98.6^\circ \text{C}$, $\vartheta_a = 25.7^\circ \text{C}$, $G_{\text{hem}} = 937.0 \text{ W}/\text{m}^2$, $G_b = 764.2 \text{ W}/\text{m}^2$, $\theta = 18.2^\circ$, $d\vartheta_m/dt = 0.51 \text{ K}/\text{h}$)

With the deployed high precision sensors, the measured/estimated power output ratio lies within +/- 3.2% for eq. A and eq. B with high probability. As can be seen from Table 3, measurement uncertainties for eq. A and eq. B are similar. A major influence on measurement uncertainty is the total tilted irradiance measurement, which stresses the importance of good radiation sensors. The low influence of the beam irradiance measurement on the overall uncertainty is due to two reasons.

- 1) For the measurement setup, the beam irradiance measurement only determines the share of beam irradiance/share of diffuse irradiance, as the diffuse irradiance is calculated as the difference of total tilted irradiance and beam irradiance ($G_d = G_{\text{hem}} - G_b$). The beam irradiance measurement does not affect the total irradiance value.
- 2) The incidence angle of the operating point is close to normal ($\theta = 18.2^\circ$), where the efficiency of diffuse/beam radiation conversion is similar for the given collector. Only if the diffuse/beam radiation conversion would be significantly different (at lower incidence angles), the beam irradiance measurement would have a substantial influence on the measurement uncertainty.

Note that the stated uncertainties apply to single measurements. As the measurement data and estimated output is averaged to 1 h intervals in the PC method, uncertainties of type A (formerly “random errors”) will be averaged out and only uncertainties of type B (formerly “systematic errors”) will remain, which can decrease the measurement uncertainty. As the extent to which the errors are of type A or type B is difficult

B-D1.1 Application of PC Method to Large Collector Arrays

to determine, it is unclear to which degree averaging will reduce the measurement uncertainty. On the other hand, installation conditions and sensor maintenance on-site will affect measurement uncertainty.

From practical experience, a major factor to keep measurement uncertainty low was the cleaning of radiation sensors. Especially the pyrhelimeter was prone to soiling because the sensor is shielded from rain by a cover.

Data recording and data filtering

On the 1 min. time grid, all explanatory variables of eq. A and eq. B were calculated if they were not measured, i.e. $(\vartheta_m - \vartheta_a)$, $(\vartheta_m - \vartheta_a)^2$, $(d\vartheta_m/dt)$, $K_b(\theta_L, \theta_T)$, as well as the collector incidence angle θ . Additionally, a binary variable was defined, indicating if internal or external shading occurred in the collector array. Furthermore, an operating signal was defined ($\dot{V}_{i,pri}/A_G > 1 \text{ l/h}\cdot\text{m}^2$). The measurement data and these additional variables were then averaged to 1 h values if all data entries were available for all 60 timesteps within an hour.^[1] Data filtering according to Table 1 for incidence angle, ambient temperature, wind velocity, hemispherical solar irradiance and beam solar irradiance was done on these hourly data, implying that 1 min. data values could be above the threshold if mean values were under it. For the criteria "no shadows" it was required that all data within the hour were without shading. For the criteria "change in collector mean temperature", the difference between maximum and minimum temperature within the hour was used, meaning that the collector mean temperatures was within a band of 5 K.^[2] Additionally, only data was used where the operating signal was true for all timestamps. Whereas this did not affect the valid data records for the four subarrays, it proved to be a useful additional check in the evaluation of other collector arrays, because it occurred that data where the collector array was not in operation for the whole hour due to a control failure was mistakenly counted as valid data. To increase comparability between the arrays, only data was selected where all operating condition restrictions were fulfilled for all subarrays at once.

Performance analysis

The performance analysis is done with a safety factor $f_{\text{safe}} = 0.92$. This makes the results comparable to the plant *Condat Paper Mill*, where the same safety factor was used. For the actual project, the performance check method was applied slightly differently.

As beam irradiance is measured for the collector array, the PC method can be applied both with eq. A and eq. B. Figure 5 shows the overview results for the measured/estimated comparison. Using the available data of the whole year 2017, a total of 199 valid data records were found for eq. A and 210 valid data records for eq. B respectively. Average specific thermal power outputs of the collector arrays were between 437.6 W/m^2

^[1] Estimating the power output with eq. A, eq. B and eq. C using (1) averaged explanatory variables or (2) averaging all measured variables and then estimating the power output could lead to slightly different results, as the collector array models are linear in the parameter, but not in the explanatory variables. Evaluations of case (1) vs. case (2) for eq. A and eq. B of the ratio of summarized estimated and summarized measured performance $d\dot{Q}\%$ for the valid data records showed no significant differences (0.004% for eq. A and 0.16% for eq. B). For eq. C, the difference could be bigger, as its non-linearity is higher.

^[2] This is more restrictive than the requirement that the average change in collector mean temperature is below 5 K/h. The criteria "change in collector mean temperature" leaves some room for interpretation.

Task 55 Towards the Integration of Large SHC Systems into DHC Networks

B-D1.1 Application of PC Method to Large Collector Arrays

and 510.1 W/m^2 for eq. A and between 430.3 W/m^2 and 502.5 W/m^2 for eq. B, showing performance differences of 14.2% and 14.3% respectively. The ranking of the collectors in terms of thermal performance and measured/estimated comparison remains the same for eq. A and eq. B. The measured/estimated comparison shows values between 95.2% and 106.1% for eq. A, and slightly better values for eq. B (using a safety factor $f_{\text{safe}} = 0.92$). Collector arrays #3 and #4 are the best in terms of thermal performance, but collector array #1 is best regarding the measured/estimated comparison.

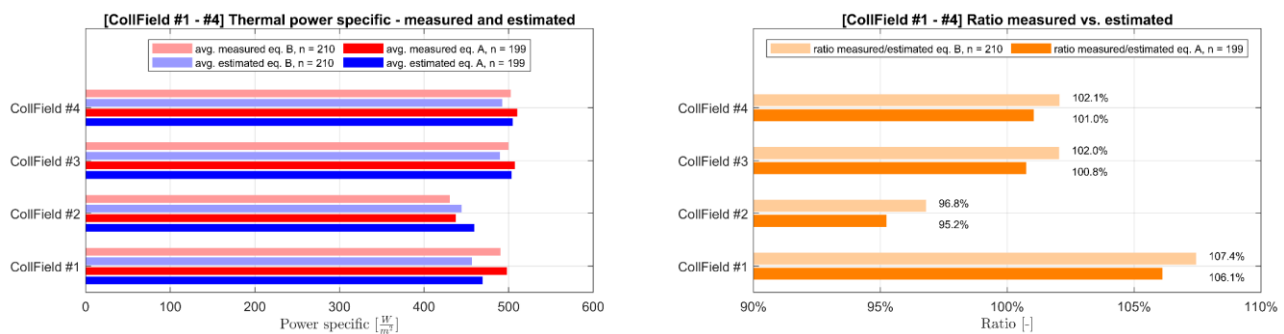


Figure 5: Measured/estimated comparison of four subarrays of plant *Fernheizwerk* with specific thermal power (left) and measured/estimated ratio (right), safety factor $f_{\text{safe}} = 0.92$

Figure 6 to Figure 9 show the retrieved evaluation points of the measured/estimated power output for collector arrays #1 - #4. Of the data records (intervals), 187 were valid both for eq. A and eq. B, whereas 12 were only valid for eq. A and 23 only for eq. B. Additional valid data records for eq. A were found around noon where beam irradiance was low, for eq. B in the morning or afternoon on clear days.

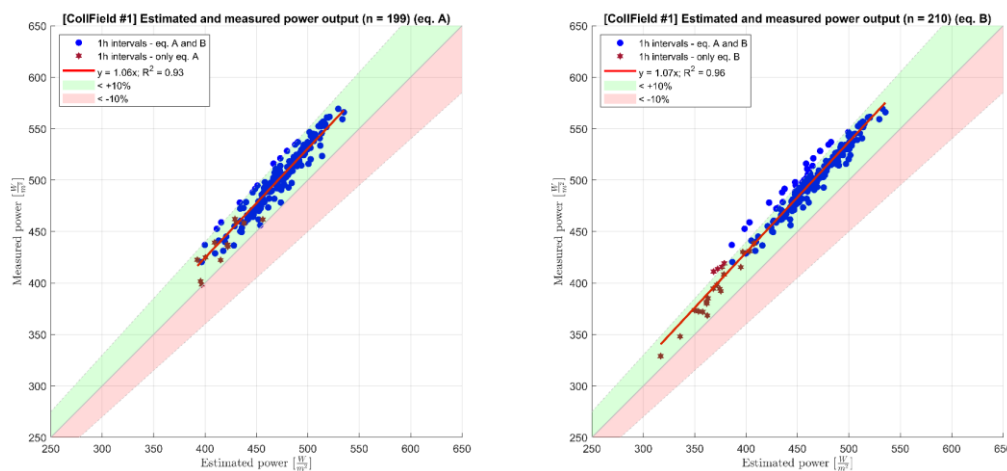


Figure 6: Estimated and measured power output (per $\text{m}^2 A_G$) of plant *Fernheizwerk*, collector array #1, safety factor $f_{\text{safe}} = 0.92$

Task 55 Towards the Integration of Large SHC Systems into DHC Networks

B-D1.1 Application of PC Method to Large Collector Arrays

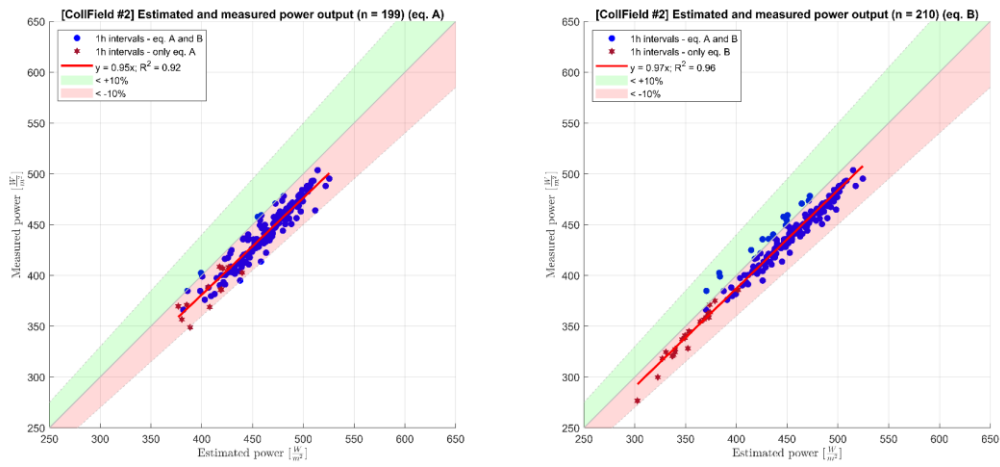


Figure 7: Estimated and measured power output (per $m^2 A_G$) of plant *Fernheizwerk*, collector array #2, safety factor $f_{safe} = 0.92$

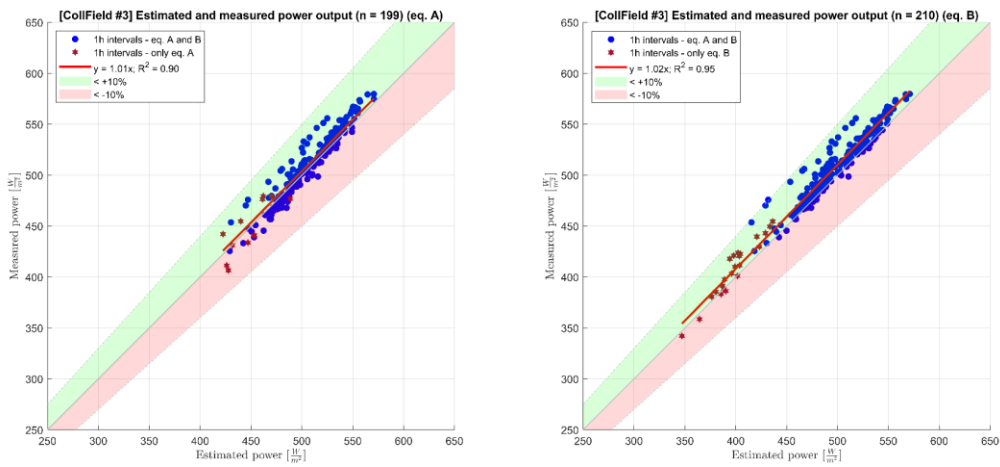


Figure 8: Estimated and measured power output (per $m^2 A_G$) of plant *Fernheizwerk*, collector array #3, safety factor $f_{safe} = 0.92$

Task 55 Towards the Integration of Large SHC Systems into DHC Networks

B-D1.1 Application of PC Method to Large Collector Arrays

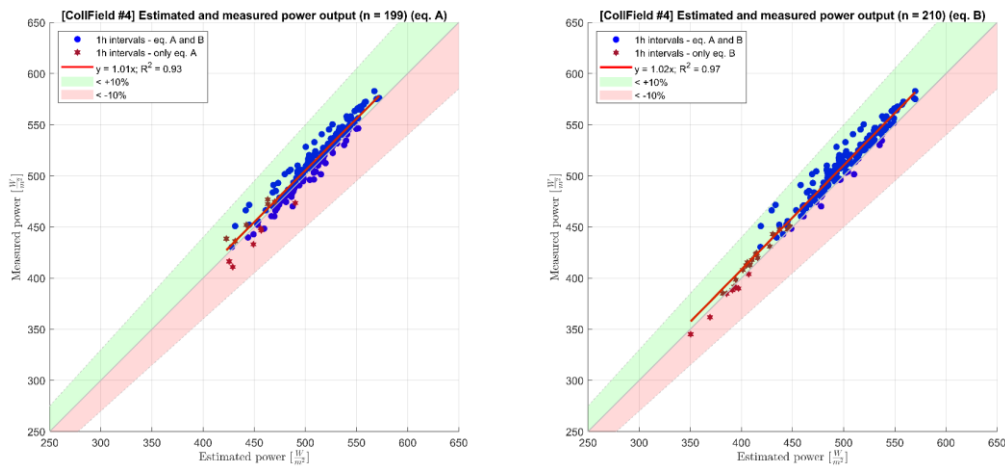


Figure 9: Estimated and measured power output (per $m^2 A_G$) of plant *Fernheizwerk*, collector array #4, safety factor $f_{safe} = 0.92$

A more detailed analysis of the spread of the valid data records for eq. A and eq. B is shown in Figure 10. For eq. B, the distribution of the measured/estimated power ratio looks less skewed, but the estimated standard deviations are similar for eq. A and eq. B. The standard deviations of all arrays are similar and only slightly higher than the measurement uncertainty.

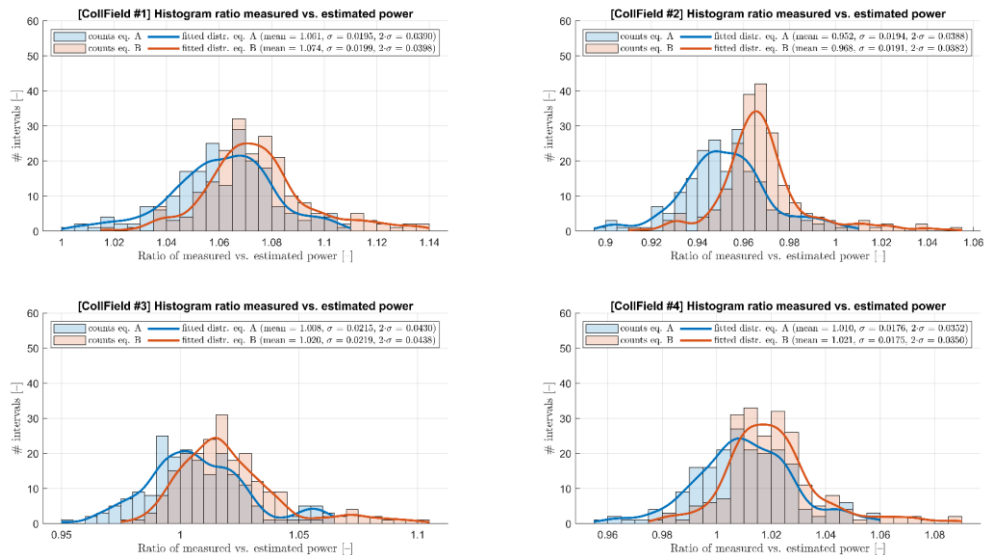


Figure 10: Histogram of measured/estimated power ratio of all valid data records for plant *Fernheizwerk*, safety factor $f_{safe} = 0.92$

The distribution of the valid data records over the year for collector array #1, eq. B is shown in Figure 11. Intervals can be found between 2017-03-24 12:00 and 2017-09-14 12:00:00. Apart from intervals of the end

Task 55 Towards the Integration of Large SHC Systems into DHC Networks

B-D1.1 Application of PC Method to Large Collector Arrays

of March and beginning of April, no apparent time trend can be seen. Further analysis brought no definitive answers regarding the reasons for the higher measured/estimated ratio in March.

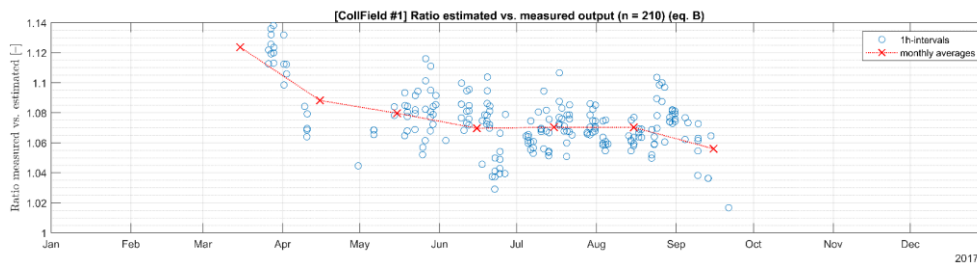


Figure 11: Time dependence of measured/estimated power ratio of plant *Fernheizwerk*, collector array #1, safety factor $f_{\text{safe}} = 0.92$

Figure 12 shows an additional analysis for collector array #1 to see if there are recognizable patterns for the measured/estimated power ratio with regard to operating conditions. Overall, there seem to be no strong patterns as to when the ratio is more favourable and when it is not. For eq. A, intervals with a higher diffuse share and a higher incidence angle seem to have a less favourable measured/estimated power ratio than the same intervals for eq. B. This may point to a bias in eq. A which does not treat beam and diffuse irradiance differently ($n_{0,\text{hem}}$ is usually calculated for diffuse share of 15%) and does not account for incidence angle effects. Measured wind speeds at the location were supposedly too low to have a significant influence on the performance and the wind sensor measured the horizontal wind speed, which might not be representative for the array.

Task 55 Towards the Integration of Large SHC Systems into DHC Networks

B-D1.1 Application of PC Method to Large Collector Arrays

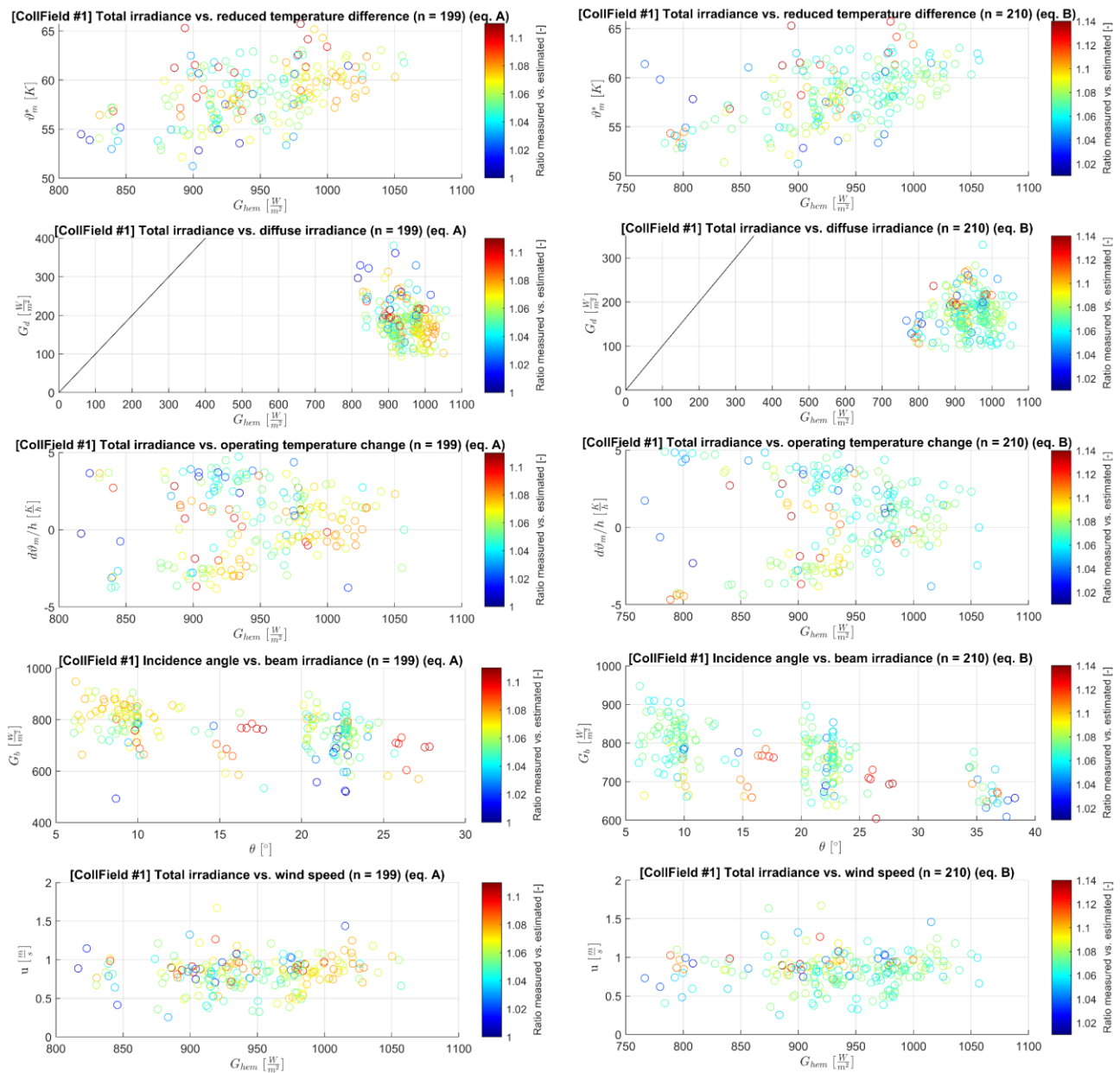


Figure 12: Measured/estimated power ratio for valid data records of eq. A and eq. B of plant *Fernheizwerk*, collector array #1, safety factor $f_{\text{safe}} = 0.92$

Figure 13 shows the measured/estimated power outputs for different interval lengths. For the selection of valid data records, the criteria “change in collector mean temperature” was adapted to the interval length, i.e. the allowed difference between maximum and minimum collector mean temperature would be $5 \text{ K} \cdot [\text{interval length}] / 1 \text{ hour}$ (e.g. 2.5 K for 30 min. intervals, 10 K for 120 min. intervals), in order to decrease the distortion of thermal capacity effects and dwelling time of the fluid through the collector array (the dwelling time was 4.3 min. on average for the valid data records for collector array #1). For sharp irradiance

Task 55 Towards the Integration of Large SHC Systems into DHC Networks

B-D1.1 Application of PC Method to Large Collector Arrays

drops and increases of the return temperature, the estimated power would overestimate the actual measurement. Interestingly, the procedure delivers similar overall results for different interval lengths, although outliers become more extreme for shorter interval lengths. Even with 120 min. interval length, a reasonable number of intervals can be found.

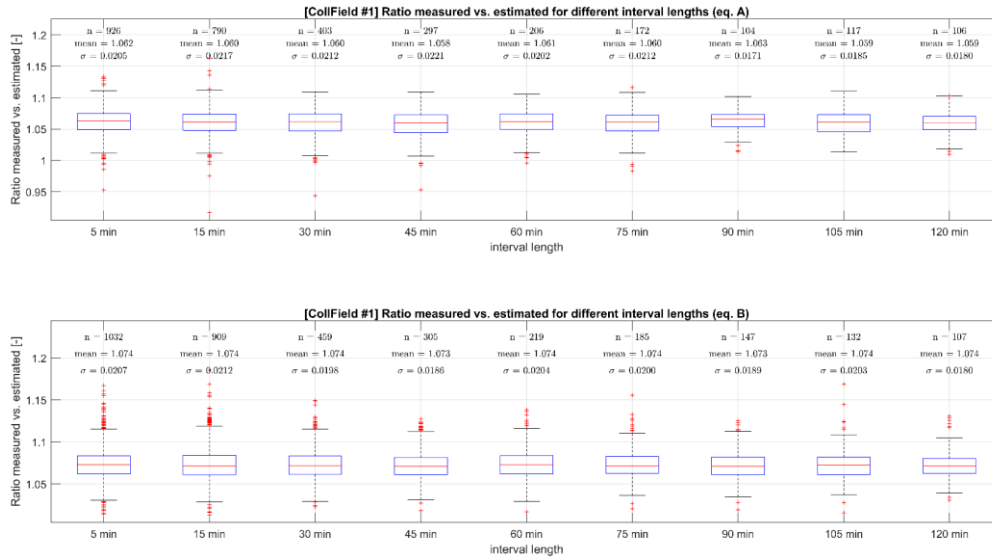


Figure 13: Evaluation with different interval lengths, plant *Fernheizwerk*, collector array #1, safety factor $f_{\text{safe}} = 0.92$

The effects of altering the restrictions on operating conditions for one subarray are analysed in Figure 14. The measured/estimated power ratio shows only small changes for different sets of restrictions. Very strict restrictions on the operating conditions make the method inapplicable, as the number of valid data records significantly decreases. Tightening restrictions on the incidence angle for eq. A to $\theta \leq 10^\circ$ would still satisfy the required number. Requiring beam levels to be $\geq 800 \text{ W/m}^2$ would significantly reduce the number of valid data records.

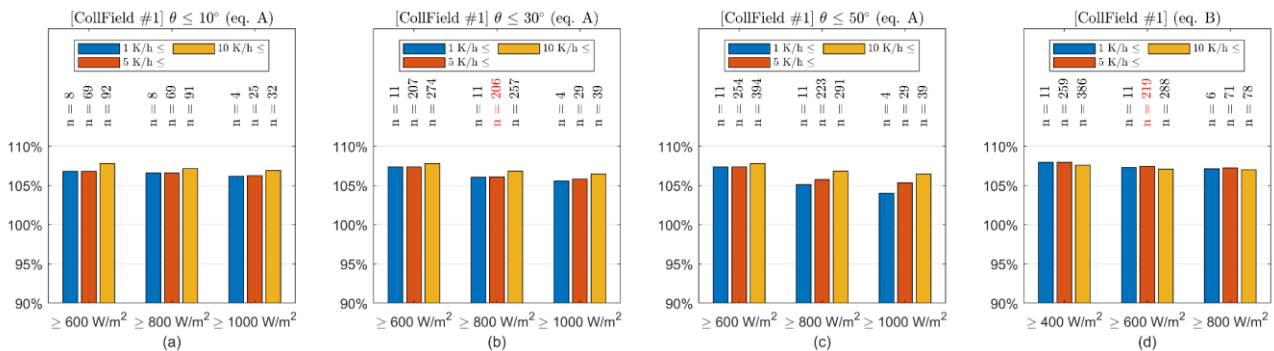


Figure 14: Evaluation with different operating conditions restrictions, plant *Fernheizwerk*, collector array #1.

Parameter Eq. A: $G_{\text{hem}} \geq 600 \text{ W/m}^2$, 800 W/m^2 , 1000 W/m^2 , angle of incidence $\leq 10^\circ$, 30° , 50° ;

Eq. B: $G_b \geq 400 \text{ W/m}^2$, 600 W/m^2 , 800 W/m^2 ; Eq. A and B: Change in collector mean temperature $\leq 1 \text{ K/h}$, 5 K/h , 10 K/h .

Red text in figures (b) and (d) show original settings of PC method

B-D1.1 Application of PC Method to Large Collector Arrays

Discussion of results

The application of the PC method to four subarrays of the plant *Fernheizwerk* proved no major difficulties. A sufficient number of valid data records (intervals) could be found. Thermal power output measurements in the collector loop and high-precision radiation sensors allowed a measurement setup comparable to ISO 9806. The measured/estimated comparison, using a safety factor $f_{\text{safe}} = 0.92$, showed values between 95.2% and 106.1% for eq. A and slightly better values for eq. B, with three out of four fields performing better than estimated. The PC method did not allow to draw a conclusion as to the reason of the deviations. The collectors deployed in the array were already in operation for 2-3 years. A probable reason for the reduced performance is soiling of the collectors, especially as smoke emitting industries are located in close proximity.

A further analysis of the valid data records showed no strong pattern as for which operating conditions the ratio of measured vs. estimated performance was higher or lower. Performance assessments with different interval lengths and filtering conditions lead to similar results. This speaks for the validity of the method. Results also indicate that for flat plate collectors, using eq. A or eq. B makes little difference. But compared to eq. A, eq. B delivers similar measured/estimated power ratios also for higher incidence angles, indicating a more balanced assessment of the collectors. An uncertainty source not mentioned in the description of the PC method is the diffuse irradiance reduction along the collector height for operating conditions with a high diffuse share. For modules within an array, lower parts typically receive less diffuse irradiance, as the sky view is obstructed by modules placed in anterior rows. A pyranometer placed on top of the collector typically overestimates the irradiance on the collectors, because the sky view is not obstructed. This effect can make a difference for plants with a narrow row spacing as *Fernheizwerk* [8].

For the application of the method, data pre-processing and quality checks consumed the major amount of time. For an easy applicability of the method, an open-source tool for data evaluation would ease the application and make data handling more transparent. Another challenge was the selection of periods without external shading. The chosen method of building a 3D model requires an additional effort. External shading is more of an issue in countries like Austria and Germany, where many large-scale solar thermal plants are located in close proximity to city buildings, than for example in Denmark, where most plants are placed in rural areas far away from the city.

Task 55 Towards the Integration of Large SHC Systems into DHC Networks

B-D1.1 Application of PC Method to Large Collector Arrays

Application to plant *Condat Paper Mill (Condat-sur-Vézère, France)*

Plant description and measurement setup

The plant data is listed in Table 4: Basic data of plant Condat Paper Mill Table 4.

Table 4: Basic data of plant *Condat Paper Mill*

<i>Overview</i>																																		
Name	Condat Paper Mill																																	
Location	Condat-sur-Vézère (France)																																	
Latitude, longitude	45.12° N, 1.23° E																																	
Operation start	January 2019																																	
Application	Preheating of the plant steam boilers make-up water																																	
System integration	A) Integration on Supply Level – A1) Heating of make-up water (according to Task 49 concepts)																																	
Plant operator	newHeat																																	
<i>Collector array</i>																																		
Collector type	flat plate collector – single-glazed with antireflective mechanical treatment																																	
Collector manufacturer	Savosolar																																	
Collector model	SF500-15																																	
Absorber type	direct flow MPE (multi port extrusion)																																	
Collector efficiency parameter (Solar Keymark)	$\eta_{0,hem}$: 0.812; $\eta_{0,b}$: 0.821; $K_a(50^\circ)$: 0.928; a_1 : 2.936 W/(K·m ²); a_2 : 0.009 W/(K ² ·m ²); a_5 : 10,200 J/(K·m ²)																																	
	<table border="1"> <thead> <tr> <th><i>Incidence angle</i></th> <th>0°</th> <th>10°</th> <th>20°</th> <th>30°</th> <th>40°</th> <th>50°</th> <th>60°</th> <th>70°</th> <th>80°</th> <th>90°</th> </tr> </thead> <tbody> <tr> <td><i>Transversal modifier $K_b(\theta_T)$</i></td> <td>1.00</td> <td>1.00</td> <td>1.00</td> <td>1.00</td> <td>0.99</td> <td>0.97</td> <td>0.91</td> <td>0.75</td> <td>0.42</td> <td>0.00</td> </tr> <tr> <td><i>Longitudinal modifier $K_b(\theta_L)$</i></td> <td>1.00</td> <td>1.00</td> <td>1.00</td> <td>1.00</td> <td>0.99</td> <td>0.98</td> <td>0.94</td> <td>0.84</td> <td>0.59</td> <td>0.00</td> </tr> </tbody> </table>	<i>Incidence angle</i>	0°	10°	20°	30°	40°	50°	60°	70°	80°	90°	<i>Transversal modifier $K_b(\theta_T)$</i>	1.00	1.00	1.00	1.00	0.99	0.97	0.91	0.75	0.42	0.00	<i>Longitudinal modifier $K_b(\theta_L)$</i>	1.00	1.00	1.00	1.00	0.99	0.98	0.94	0.84	0.59	0.00
<i>Incidence angle</i>	0°	10°	20°	30°	40°	50°	60°	70°	80°	90°																								
<i>Transversal modifier $K_b(\theta_T)$</i>	1.00	1.00	1.00	1.00	0.99	0.97	0.91	0.75	0.42	0.00																								
<i>Longitudinal modifier $K_b(\theta_L)$</i>	1.00	1.00	1.00	1.00	0.99	0.98	0.94	0.84	0.59	0.00																								
Collector gross area	15.96 m ²																																	
Total gross collector area	4,212 m ² (264 collectors)																																	
Slope	variable (single-axis tracking, rotational axis oriented North-South, tracking range of $\pm 44^\circ$)																																	
Orientation	$\gamma = -90^\circ$																																	
Row spacing	5.8 m																																	
Fluid	primary loop: 30% propylene glycol, secondary loop: demineralized water (used for performance assessment)																																	
<i>Measurement setup</i>																																		
	<i>Brand / Type</i>	<i>Type</i>	<i>Uncertainty</i>	<i>Level I / II (of PC method)</i>																														
Volume flow (secondary side)	Ultrasonic flow sensor Kamstrup ULTRAFLOW® 34		< 1.5%	I																														
Fluid temperature	Resistance Thermometer Baumer Pt100	Class B	+/- 0.8 K	none																														
Fluid properties	density: 990 kg/m ³ , heat capacity: 4.18 kJ/kg·K																																	
Thermal power	Kamstrup MULTICAL® 602 in connection with Kamstrup ULTRAFLOW® 34 and Baumer PT100	Class B	< 2.0%	I																														
Ambient temperature	not specified			none																														
Total radiation in collector plane	Pyranometer Kipp & Zonen SMP 21	Class A		I																														

Task 55 Towards the Integration of Large SHC Systems into DHC Networks

B-D1.1 Application of PC Method to Large Collector Arrays

Beam radiation (DNI)	Pyrheliometer Kipp & Zonen SHP1 (mounted on Kipp & Zonen SOLSYS 2 sun tracker)	Class A	I
Wind speed (horizontal)	Integrated in the tracking system		
Data logging	PLC Phoenix Contact - ILC 390 PN 2TX-IB – 2985314; 2-wire PT100 with integrated 4-20 mA transmitter connection to temperature sensors		
Sampling rate	Hourly average based on 2 sec. sampling rate		
Measurement quality assurance	regular on-site inspection of measurement equipment, regular cleaning of radiation sensors, automated checks for data transmission, missing data and physically implausible values, documentation of all plant events (e.g. power supply interruption, maintenance work, etc.)		

Data evaluation

Measurement period	2020-01-03 to 2020-09-09
Evaluation tool	Excel
Used equation for PC method	eq. A, eq. B
Evaluation performed by	newHeat

The Condat solar thermal plant supplies heat to the paper mill of Condat-sur-Vézère in Dordogne. The heat is used to preheat the make-up water of the steam gas boilers (from 20 to 90°C). This plant was until 2021 the largest solar thermal plant in France. Also, it is the world’s first plant using flat plate collectors with tracking systems. Here are some figures:

- Peak solar power: 3.4 MW_{th}
- Surface area of solar collectors: 4,212 m²
- Heat storage capacity: 500 m³
- Annual energy delivered: around 3,900 MWh_{th}/year

Figure 15 shows pictures of the plant.



Figure 15 : Pictures of the plant *Condat Paper Mill*. Source: newHeat

B-D1.1 Application of PC Method to Large Collector Arrays

Data handling and uncertainties

Internal and external shading

The row spacing in Condat is relatively wide (5.8 m). This is because a tracking system needs more space than fixed collectors to be able to rotate around its N-S axis. The internal shadow in the Condat solar field is first depending on the sun position across the day, but also depending on the varying tilt angle of the collectors. To select data without internal shading, a specific formula considering solar positions and tilt angle determines whether loops would shade each other for every hour or not. This formula is detailed in the ISO Collector fields – Check Performance [5].

Firstly, the *shading angle* (ideal tracking angle after which no reciprocal shadows occur) had to be calculated:

$$\beta_{sh} = \tan^{-1} \left(\sqrt{\frac{S^2}{W^2} - 1} \right) = \tan^{-1} \left(\sqrt{\frac{5.8^2}{2.58^2} - 1} \right) \approx 63,6^\circ$$

On the equation above S represents the collector row spacing center-to-center and W the width of a collector. Here, β_{sh} is superior to the maximum tracking range, β_{max} , of Condat (44°). It means that reciprocal shading always stops in the morning before the tracker rotation begins and starts in the afternoon after the tracker reached its maximum tilt to the West.

According to ISO:24194 [5], if $\beta_{max} < \beta_{sh}$, the inequation below must be verified for the no-shadow condition to be true for the concerned data points:

$$\left| \frac{\tan(h)}{\cos(\gamma_s - \gamma)} \right| \geq \frac{\sin(\beta_{max})}{\frac{S}{W} - \cos(\beta_{max})}$$

γ represents the collector surface azimuth angle and β_{max} is the tracking range. Here $\gamma = -90^\circ$ and $\beta_{max} = 44^\circ$.

On the selected period (March to September), this internal shading condition is verified more than 74.3% of the time during supply periods.

Regarding external shading, it is inexistant on the solar field because the area on which collectors have been placed was a landfill that has been rehabilitated. Therefore, no external shading has been considered.

Overall filtering for valid data record selection

According to the criteria established in Table 1, the following criteria were checked for each available point:

- No shadows (according to the above-mentioned method)
- Incidence angle $< 30^\circ$ for eq. A and no restrictions on the incidence angle for eq. B
- Change in collector mean temperature over the hour < 5 K
- Wind velocity ≤ 10 m/s
- $G_{hem} > 800$ W/m² for eq. A and $G_b \geq 600$ W/m² for eq. B

Task 55 Towards the Integration of Large SHC Systems into DHC Networks

B-D1.1 Application of PC Method to Large Collector Arrays

All these conditions were cross-checked with an Excel-based spreadsheet analysis. The valid data records kept for the performance check exclusively verify all these conditions simultaneously.

Uncertainties and associated safety factor

With the collector manufacturer, who acted as a turnkey supplier for this project, a safety factor of $f_{\text{safe}} = 0.92$ was agreed on for eq. A and eq. B to cover the three types of uncertainties, namely heat losses from pipes f_p , measurement uncertainties f_U and other uncertainties f_O . High-precision sensors were used for the volume flow and radiation measurement. The temperature sensors were Class B sensors with a higher uncertainty than required by the PC method ($< 0,35$ K).

Performance analysis

As beam irradiance is measured for the collector array, the PC method can be applied both with eq. A and eq. B. Figure 16 and Figure 17 show the estimated and measured power output for the valid data records, using eq. A and eq. B respectively.

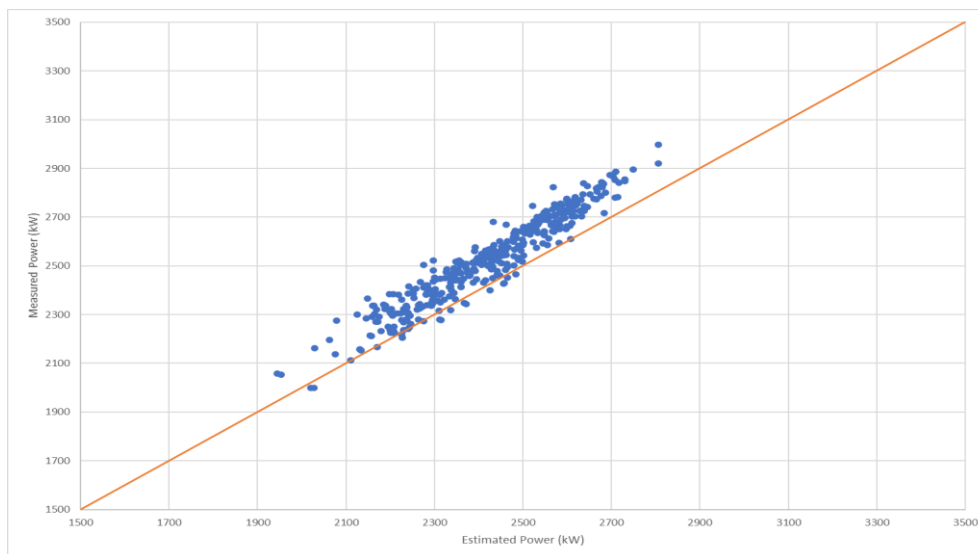


Figure 16: Estimated and measured power output of plant *Condat Paper Mill*, eq. A, $n = 397$, safety factor $f_{\text{safe}} = 0.92$

Task 55 Towards the Integration of Large SHC Systems into DHC Networks

B-D1.1 Application of PC Method to Large Collector Arrays

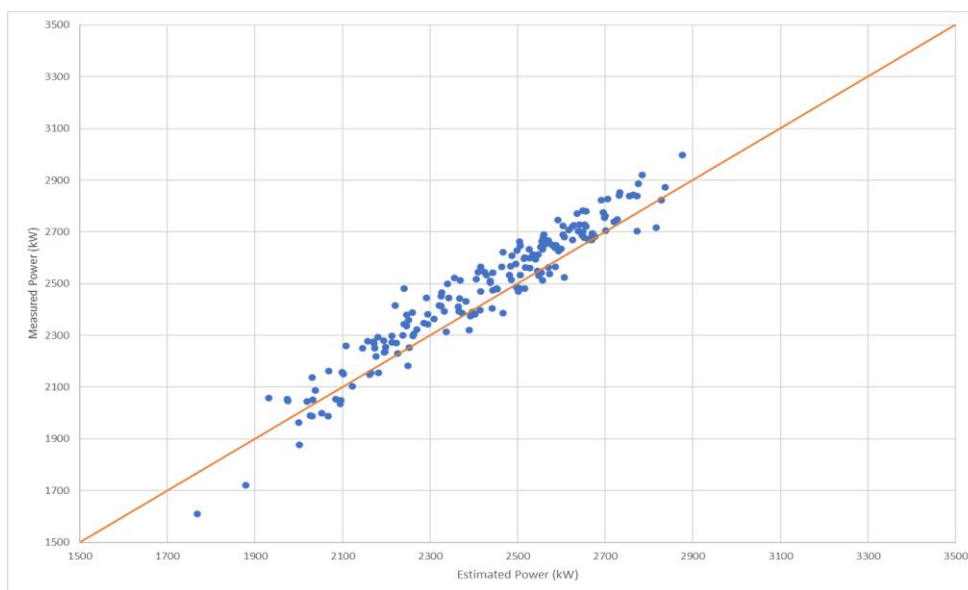


Figure 17: Estimated and measured power output of plant *Condat Paper Mill*, eq. B, $n = 186$, safety factor $f_{safe} = 0.92$

Table 5 summarizes the results for eq. A and eq. B.

Table 5: Results for eq. A and eq. B for *Condat Paper Mill*

	Eq. A	Eq. B
Number of data records (1h intervals)	4557	2902
Number of valid data records (1h intervals)	397	186
Measured average power for valid data records	2525.9 kW	2478.3 kW
Estimated average power for valid data records	2421.8 kW	2423.8 kW
Ratio measured/estimated for valid data records	1.04	1.02
Safety factor f_{safe}	0.92	0.92
Estimate is verified	yes	yes

From the start of the evaluation period (2020-03-01), the first 20 valid data records needed for the performance check using eq. A were available on 2020-05-15, after 2.5 months of measurement. Using eq. B, the first 20 valid data records were available on 2020-03-28, after 1 month of measurement. Over one month during the summer period (2020-05-16 to 2020-06-13) the number of valid points was exactly the same. During the summer it was possible to obtain 20 points in around 4-5 days. As stated in Table 5, the number of data records (1h intervals) is 4557 for eq. A and 2902 for eq. B. This deviation is due to the fact that the pyrheliometer which measures the beam irradiance (which is necessary for eq. B) was not installed for the entire evaluation period.

Task 55 Towards the Integration of Large SHC Systems into DHC Networks

B-D1.1 Application of PC Method to Large Collector Arrays

Figure 18 shows the average measured and estimated powers for eq. B (left) and eq. A (right).

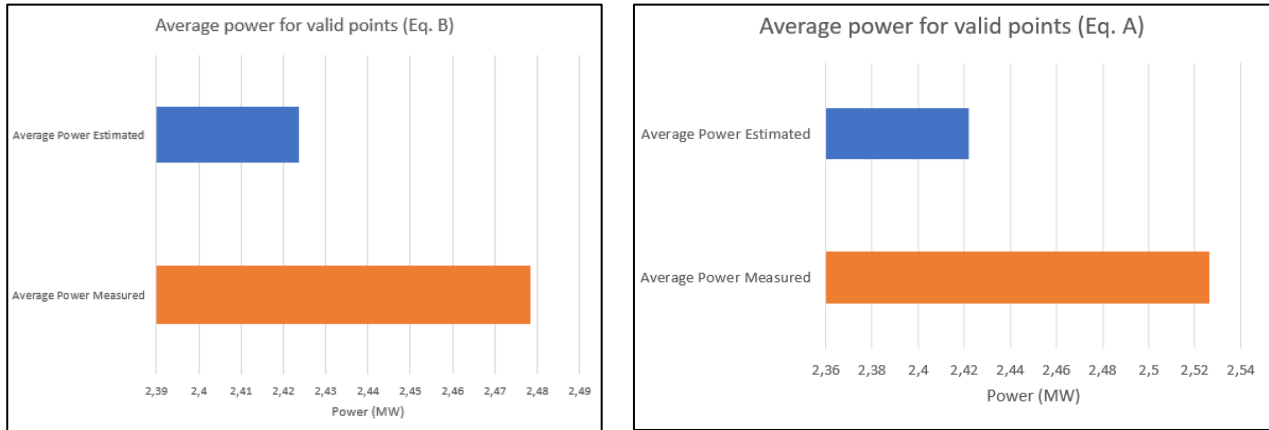


Figure 18 : Plots of average measured powers and corresponding estimated average powers for eq. B (left) and eq. A (right)

These plots visually illustrate that in both cases the PC is verified because:

$$\text{Average}[P_{\text{meas}}] \geq \text{Average}[P_{\text{estimate}}]$$

Discussion of results

The application of the PC method to the plant *Condat Paper Mill* showed, that the performance check (with a safety factor $f_{\text{safe}} = 0.92$) was achieved with both equations. Results for eq. A and eq. B regarding the ratio of measured/estimated performance was similar, but the required 20 valid data records could be obtained faster with eq. B in spring compared to eq. A.

B-D1.1 Application of PC Method to Large Collector Arrays

Conclusion and outlook

This fact sheet describes the application of the PC method to two large-scale solar thermal plants with flat plate collectors, namely the plants *Fernheizwerk* and *Condat Paper Mill*. The following conclusions can be drawn:

- For both plants, the application of the PC method was straightforward and proved no major difficulties.
- For three out of four evaluated collector arrays of the plant *Fernheizwerk* and for the plant *Condat Paper Mill*, the measured performance exceeded the estimated performance (using a safety factor of $f_{\text{safe}} = 0.92$).
- For both plants, eq. A and eq. B gave similar results for the ratio of the measured and estimated performance with differences in the range of 1-2%. In summer, the required 20 intervals can be obtained within 4-5 clear days. The required intervals were faster to obtain with eq. B.
- A major factor to keep measurement uncertainty low is the regular cleaning of the radiation sensors.
- An additional analysis for the plant *Fernheizwerk* showed that the ratio of measured and estimated performance had a measurement uncertainty of $\pm 3.2\%$ (2σ) for eq. A and B, based on data sheet specifications of the deployed sensors (the plant has high-precision measurement equipment installed). The distribution of the ratios of measured and estimated performance for the valid data records had similar 2σ -levels.
- For the plant *Fernheizwerk*, the averaging interval of the data records varying between 5 min. and 120 min. (instead of hourly average values) and minor modifications of the operating condition restrictions did not alter the overall performance assessment to a large extend.
- For the plant *Fernheizwerk*, the level of the measured/estimated power ratio showed no clear recognizable pattern regarding operating conditions for the valid data records. This indicates, that the performance assessment does not have a systematic bias regarding the specifics of the valid data records, e.g. different assessments for lower vs. higher beam irradiance levels or lower vs. higher operating temperatures.

For future applications and developments of the PC method, the following recommendations are worth considering:

- For most plants with flat plate collectors, the global tilted irradiance is measured, but not the beam radiation. Allowing the beam and diffuse irradiance being calculated with a radiation model, splitting the measured global tilted irradiance, would make it possible to use eq. B, where the required intervals for the performance check could be obtained faster.
- Measurement data of wind velocity is required to check the operating condition restrictions (wind velocity ≤ 10 m/s). In regions where high wind velocities are very rare, like Austria, many plants do not have a wind sensor installed. For these regions, having the option to use other data, e.g. of nearby weather stations, to indicate that the wind velocity is low, would ease the application of the method.
- The PC method did not allow to draw conclusions as to why and when the measured power output of the collector array was higher or lower than the estimated power output. As the PC method is easy applicable, it can be used for quick and low-cost on-going surveillance. If performance reductions

Task 55 Towards the Integration of Large SHC Systems into DHC Networks

B-D1.1 Application of PC Method to Large Collector Arrays

over time or high deviations of measured and estimated power output are detected, a further analysis can be done with additional collector array test methods (e.g. [8], [17]), which are able to derive collector parameters, showing where the deviations could come from.

- On the other hand, the straightforward and easy to apply nature of the PC method, coupled with a clear acceptance criterion, makes it an ideal candidate for structuring the reception process between a solar field supplier and its client during commissioning and the following months.
- One of the most time-consuming steps in the application of the PC method is the data pre-processing and quality check of measurement data. A publicly available open-source software tool to process monitoring data of large-scale solar thermal plants to ease data processing steps would be desirable.

Task 55 Towards the Integration of Large SHC Systems into DHC Networks

B-D1.1 Application of PC Method to Large Collector Arrays

Nomenclature

Symbol	Description	Unit
A_G	Gross area of collector as defined in ISO 9488	m^2
a_1	Collector heat loss coefficient at $(\vartheta_m - \vartheta_a) = 0$ K	$W/(m^2 \cdot K)$
a_2	Temperature dependence of collector heat loss coefficient	$W/(m^2 \cdot K^2)$
a_5	Effective thermal capacity of collector	$J/(m^2 \cdot K)$
a_8	Radiation losses of collector	$W/(m^2 \cdot K^4)$
b_0	incidence angle modifier (IAM) parameter for b_0 equation	-
$C_{f, pri}$	Specific heat capacity of heat transfer fluid in solar circuit at solar circuit mean temperature	$J/(kg \cdot m^2)$
$C_{f, sec}$	Specific heat capacity of heat transfer fluid (water) in secondary side at heat exchanger mean temperature	$J/(kg \cdot m^2)$
f_{safe}	Safety factor, taking into account pipe and other heat losses, measurement uncertainties and other uncertainties	-
G_b	Direct solar irradiance on collectors	W/m^2
G_d	Diffuse solar irradiance, measured at the top of collector	W/m^2
G_{hem}	Hemispherical solar irradiance, measured at the top of collector	W/m^2
$K_b(\theta_L, \theta_T)$	Incidence angle modifier for direct solar radiation	-
K_d	Incidence angle modifier for diffuse solar radiation	-
$\dot{Q}_{pri, meas}$	Measured thermal power of collector array on primary side	W
$\dot{Q}_{sec, meas}$	Measured thermal power of collector array, supplied at heat exchanger on secondary side	W
$\dot{Q}_{pri, est}$	Estimated thermal power of collector array on primary side	W
$\dot{Q}_{sec, est}$	Estimated thermal power of collector array, supplied at heat exchanger on secondary side	W
S	Collector rows spacing, center to center	m
t	Time	s
u	Surrounding air speed	m/s
W	Collector width	m
$\dot{V}_{i, pri}$	Volume flow at collector array inlet in solar circuit	m^3/s
$\dot{V}_{i, sec}$	Volume flow at heat exchanger inlet on secondary side	m^3/s
β_{sh}	Tracker ideal shading angle	
β_{max}	Tracker maximum range	
$\eta_{0, b}$	Peak collector efficiency ($\eta_{0, b}$ at $\vartheta_m - \vartheta_a = 0$ K) based on beam irradiance G_b	-
$\eta_{0, hem}$	Peak collector efficiency ($\eta_{0, hem}$ at $\vartheta_m - \vartheta_a = 0$ K) based on hemispherical irradiance G_{hem}	-
γ	Collector surface azimuth angle	degrees
θ	Angle of incidence	degrees
θ_L	Longitudinal angle of incidence: angle between the normal to the plane of collector and incident sunbeam projected into the longitudinal plane	degrees
θ_T	Transversal angle of incidence: angle between the normal to the plane of collector and incident sunbeam projected into the transversal plane	degrees
ϑ_a	Ambient air temperature	$^{\circ}C$
$\vartheta_{i, sec}$	Heat exchanger inlet temperature, measured in secondary loop at heat exchanger inlet	$^{\circ}C$
$\vartheta_{e, sec}$	Heat exchanger outlet temperature, measured in secondary loop at heat exchanger outlet	$^{\circ}C$
ϑ_m	Mean temperature of heat transfer fluid in collector loop	$^{\circ}C$
$\rho_{i, pri}$	Density of heat transfer fluid at collector array inlet in solar circuit	kg/m^3
$\rho_{i, sec}$	Density of heat transfer fluid at heat exchanger inlet temperature on secondary side	kg/m^3
σ	Standard deviation	-

B-D1.1 Application of PC Method to Large Collector Arrays

References

- [1] D. Tschopp, Z. Tian, M. Berberich, J. Fan, B. Perers, and S. Furbo, "Large-scale solar thermal systems in leading countries: A review and comparative study of Denmark, China, Germany and Austria," *Applied Energy* 270 (114997), 2020, <https://doi.org/10.1016/j.apenergy.2020.114997>
- [2] S. Fahr, D. Tschopp, J. E. Nielsen, K. Kramer, and P. Ohnewein, "Review of in situ Test Methods for Solar Thermal Installations," *Proceedings ISES Solar World Congress 2019*, 2019, <https://doi.org/10.18086/swc.2019.06.02>
- [3] J. E. Nielsen and D. Trier, "Guaranteed power output. IEA-SHC TECH SHEETS 45.A.3.1. Available online: <http://task45.iea-shc.org/fact-sheets>", 2014.
- [4] J. E. Nielsen, "Guarantee of annual output. IEA-SHC TECH SHEET 45.A.3.2. Available online: <http://task45.iea-shc.org/fact-sheets>", 2014.
- [5] ISO/TC 180/SC (ISO/DIS 24194) Solar energy - Collector fields - Check of Performance. Version 11.0, 2020.
- [6] EN ISO 9806 Solar energy — Solar thermal collectors — Test methods, 2017.
- [7] P. Ohnewein, D. Tschopp, M. Hamilton-Jones, and H. Schrammel, *ADA Advanced Data Analysis*. AEE INTEC, 2017.
- [8] P. Ohnewein, D. Tschopp, R. Hausner, and W. Doll, "Dynamic Collector Array Test (D-CAT). Final Report FFG Project 848766 - MeQuSo. Development of methods for quality assessment of large-scale solar thermal plants under real operating conditions. Available online: <https://www.aee-intec.at/Uploads/dateien1538.pdf>," AEE - Institute for Sustainable Technologies, Gleisdorf, 2020.
- [9] B. Perers, H. Zinko, and P. Holst, *Analytical model for the daily energy input output relationship for solar collector systems*. Stockholm: Swedish Council for Building Research, 1985.
- [10] J. A. Duffie, W. A. Beckman, and N. Blair, *Solar Engineering of Thermal Processes, Photovoltaics and Wind*. John Wiley & Sons, 2020.
- [11] J. Appelbaum and J. Bany, "Shadow effect of adjacent solar collectors in large scale systems," *Solar Energy*, vol. 23, no. 6, pp. 497–507, 1979, [https://doi.org/10.1016/0038-092X\(79\)90073-2](https://doi.org/10.1016/0038-092X(79)90073-2)
- [12] M. Fährnich, "Messen und Testen von Solarkollektorfeldern. Verhalten, Unsicherheiten und Abhängigkeiten von relevanten physikalischen Messgrößen im Solarkollektorfeld und deren Auswirkungen auf die Wärmeleistungsbestimmung," Master thesis, Karl-Franzens-Universität, Graz, 2018.
- [13] GIS-Steiermark. <https://gis.stmk.gv.at> (accessed Nov. 24, 2017).
- [14] P. Ohnewein, R. Hausner, and D. Preiß, "ParaSol, Hydraulikdesign von parallelen Kollektormodulen in solarthermischen Großanlagen. Final project report." AEE INTEC, 2015.
- [15] ISO/IEC Guide 98-3:2008, *Uncertainty of measurement - Part 3: Guide to the expression of uncertainty in measurement*. Geneva: ISO, 2008.
- [16] A. Zirkel-Hofer *et al.*, "Improved in situ performance testing of line-concentrating solar collectors: Comprehensive uncertainty analysis for the selection of measurement instrumentation," *Applied Energy* 184, pp. 298–312, 2016, <https://doi.org/10.1016/j.apenergy.2016.09.103>
- [17] W. Kong, S. Furbo, and B. Perers, "Development and validation of an in situ solar collector field test method," DTU, Kgs. Lyngby, 2019.